Determining the molecular Huang-Rhys factor via scanning-tunneling-microscopy–induced luminescence

Fei Wen
Graduate School of China Academy of Engineering Physics, Beijing 100084, China

Guohui Dong*
College of Physics and Electronic Engineering, Sichuan Normal University, Chengdu 610068, China

(Received 17 November 2023; accepted 26 March 2024; published 17 April 2024)

Scanning-tunneling-microscopy–induced luminescence can be used to probe the optical and electronic properties of molecules. Concerning the vibronic coupling, we model the molecule as a two-level system with vibrational degrees of freedom. Based on Bardeen's theory, we express the inelastic tunneling current in terms of the Huang-Rhys factor within the inelastic electron scattering mechanism. We find that the differential conductance, varying with the bias voltage, exhibits a distinct step structure with various vibronic coupling strengths. The second derivative of the inelastic tunneling current with respect to the bias voltage shows the characteristics of a vibrational-level structure with the Franck-Condon factor. Consequently, we propose a method to determine the Huang-Rhys factor of molecules, holding promising potential within the realm of solid-state physics.

DOI: 10.1103/PhysRevA.109.042817

I. INTRODUCTION

Scanning-tunneling-microscopy–induced luminescence (STML) serves as a powerful tool for detecting various molecular properties, including molecular conformation [1,2] and spectral characteristics [1–6]. Researchers have made substantial progress in understanding the fine structures of molecular energy by combining the current-voltage characteristics of molecular junctions with optical spectroscopy [7–12]. Intramolecular transitions with vibronic features have also been successfully detected in the differential conductance spectra at the threshold of vibrational mode energy [2,13–18].

In 1950, Huang and co-workers derived the expression for the Huang-Rhys factor (denoted as S) which characterizes the strength of the vibronic coupling [19]. The critical importance of the Huang-Rhys factor was confirmed in both theory and experiments [20–23]. Although a simple model which assumes that all vibration modes have the same frequency under the Born-Oppenheimer approximation is used, in many practical applications, the results derived from this single-mode model using the equal-mode approximation [24] have been proven to be the most useful. There are several ways to determine the Huang-Rhys factor in experiments, such as fitting the spectrum and extracting S from the Stokes shift. However, these methods often require accurate spectral shapes and higher resolution, which can be challenging to achieve in practice [25]. Taking advantage of the low temperature and excellent accuracy of STML, measuring the Huang-Rhys factor becomes a more accessible task.

In general, the luminescence is induced by STM with three mechanisms: the inelastic electron scattering (IES) mechanism [26,27], the charge injection (CI) mechanism [2,9,28–31], and the plasmon mechanism [10,32–35]. Here, we specifically focus on the IES mechanism, where electrons tunnel inelastically from one electrode to another, exciting the molecule in the gap between the tip and the substrate. Taking the vibronic coupling into account, we calculate the inelastic tunneling current based on the perturbation theory [36]. The inelastic tunneling current is expressed in terms of the Franck-Condon factor which describes the square of the overlap integral between the vibrational wave functions of the two states that are involved in the transition. The Franck-Condon factor is written in the form of the Huang-Rhys factor [37,38], which is determined through the second derivative of the inelastic tunneling current with respect to the bias voltage.

The rest of the paper is organized as follows. In Sec. II, we describe the Hamiltonian of our model in which the molecule is treated as a two-level system with the vibrational degrees of freedom. Then, we derive the inelastic tunneling current in terms of the Huang-Rhys factor. Section III shows the inelastic tunneling current, the differential conductance, and the second derivative of the inelastic tunneling current with respect to the bias voltage as a function of the bias voltage. Finally, we summarize the main contributions in Sec. IV.

II. MODEL AND METHOD

A. Hamiltonian

The STML system comprises a metallic tip, a molecular sample, a decoupling layer, and a metallic substrate. The decoupling layer serves to separate the molecule from the

*Corresponding author: 20210076@sicnu.edu.cn

substrate, blocking the quenching process and enabling the molecular luminescence. In the IES mechanism, when a bias voltage is applied between the tip and substrate, electrons tunnel from one electrode to another, thereby exciting the molecule.

The total Hamiltonian is divided into three components: the electronic Hamiltonian, the molecular Hamiltonian, and the interaction Hamiltonian. The electronic component is solved using Bardeen's theory. The molecular aspect is simplified as a two-level system with vibrational degrees of freedom. The interaction between the electron and the molecule is the Coulomb interaction.

Based on Bardeen's theory, it is assumed that the tip and the substrate are separated from each other. The stationary Schrödinger equations are

$$\hat{H}_t|\phi_k\rangle = \tilde{\xi}_k|\phi_k\rangle, \tag{1}$$

$$\hat{H}_s|\varphi_n\rangle = \tilde{E}_n|\varphi_n\rangle, \tag{2}$$

where $\hat{H}_t$ and $\hat{H}_s$ represent the Hamiltonians of electrons in the tip and the substrate, respectively. ϕ_k and φ_n are the electronic wave functions of the corresponding regions. $\tilde{\xi}_k$ and $\tilde{E}_n$ are the energies of the tunneling electrons located at the tip and the substrate region when the bias voltage V_b is applied between the electrodes. $\tilde{\xi}_k$ and $\tilde{E}_n$ are expressed in terms of the electronic energy in the absence of the bias voltage,

$$\tilde{\xi}_k = \xi_k + eV_b, \tag{3}$$

$$\tilde{E}_n = E_n, \tag{4}$$

where ξ_k (E_n) is the energy of the tunneling electron at the tip (substrate) region when the bias is zero. e represents the elementary charge of an electron. Selecting the center of the molecule as the origin of the coordinates, the wave functions in Eqs. (1) and (2) are explicitly written as

$$\phi_k(\vec{r}) = A_k \frac{e^{-\kappa_k(|\vec{r}-\vec{a}|-R)}}{\kappa_k|\vec{r}-\vec{a}|}, \tag{5}$$

$$\varphi_n(\vec{r}) = B_n e^{-\kappa_n|z|}, \tag{6}$$

in which A_k and B_n are the normalized coefficients. $\vec{r}$ represents the position of the tunneling electron. $|z|$ denotes the distance between the tunneling electron and the substrate. The apex of the tip is assumed to be a sphere. The coordinates of the center and the radius of curvature are denoted as $\vec{a}$ and R. κ_k and κ_n are the decay constants and can be expressed as

$$\kappa_k = \frac{\sqrt{-2m_e\xi_k}}{\hbar}, \tag{7}$$

$$\kappa_n = \frac{\sqrt{-2m_eE_n}}{\hbar}, \tag{8}$$

in which m_e represents the mass of the electron and $\hbar$ is the reduced Planck constant.

The molecule is modeled as a two-level system with the vibrational degrees of freedom. The molecular Hamiltonian is

$$\hat{H}_m = (E_g + \nu\hbar\omega)|g,\nu\rangle\langle g,\nu| + (E_e + \nu'\hbar\omega)|e,\nu'\rangle\langle e,\nu'|, \tag{9}$$

where ω is the frequency of the vibration. E_g and $\nu\hbar\omega$ (E_e and $\nu'\hbar\omega$) represent the electronic energy and the vibrational energy associated with the ground (excited) state of the molecule. $|g\rangle$ represents the ground state of the molecular electron, while $|e\rangle$ corresponds to the excited state. $|\nu\rangle$ ($|\nu'\rangle$) is the vibrational state with the ground (excited) state of the molecule.

The interaction between the tunneling electron and the molecule is approximated as the electron-dipole interaction [26],

$$\hat{H}_{el\text{-}m} = -e\frac{\vec{r}\cdot\vec{\mu}}{|\vec{r}|^3}, \tag{10}$$

where $\vec{\mu}$ is the molecular dipole.

B. The Franck-Condon factor

Within the Born-Oppenheimer approximation, the total wave function of the molecule is expressed as the product of the electronic wave function and the vibrational wave function. For the treatment of molecular vibrations, the harmonic approximation is often employed. The Hamiltonian of the nuclear vibration takes the form of a harmonic oscillator [19] with the characteristic frequency ω. The ground states of vibrational states $|\nu\rangle$ and $|\nu'\rangle$ can be expressed as $|0_g\rangle$ and $|0_e\rangle$, respectively. The subscript g and e indicate the electronic ground state and excited state that couple with vibrational states. In the molecular excited state, the harmonic oscillation is viewed as a translation of the harmonic oscillator when the molecule is in the ground state, thus we establish the following relationship,

$$|0_e\rangle = \hat{D}(\alpha)|0_g\rangle, \tag{11}$$

in which $\hat{D}(\alpha)$ is the translation operator, capable of translating the harmonic oscillator by a distance of q in real space.

$$q = \alpha\sqrt{\frac{2\hbar}{m_n\omega}}, \tag{12}$$

where m_n is the mass of the harmonic oscillator. The Franck-Condon factor describes the overlap of the vibrational wave functions in the molecular ground state and the molecular excited state. It is expressed as follows:

$$F_{\nu\nu'} = |\langle\nu|\nu'\rangle|^2. \tag{13}$$

Due to the low temperature of the experiment, the vibrational state associated with the electronic ground state is assumed to be in its ground state, i.e., $|\nu\rangle = |0_g\rangle$. Then, the Franck-Condon factor is simplified as

$$|\langle 0_g|\nu'\rangle|^2 = e^{-S}\frac{S^{\nu'}}{\nu'!}, \tag{14}$$

where S is the Huang-Rhys factor and it can be expressed as

$$S = |\alpha|^2 = q^2\frac{m_n\omega}{2\hbar}. \tag{15}$$

C. The inelastic tunneling current

At the initial time, we assume that the tunneling electron is located in the substrate region and the molecule is in the electronic and vibrational ground state due to the low temperature

in experiments. We express the state of the system at time t as

$$|\Psi(t)\rangle = e^{-i(\tilde{E}_n+E_g+\nu\hbar\omega)t/\hbar}|g,\nu\rangle|\varphi_n\rangle + \sum_{k,\nu} c_{g\nu k}(t)|g,\nu\rangle|\phi_k\rangle + \sum_{k,\nu'} c_{e\nu' k}(t)|e,\nu'\rangle|\phi_k\rangle, \quad (16)$$

where $|\nu\rangle = |0_g\rangle$. $c_{g\nu k}$ represents the elastic tunneling amplitude, while $c_{e\nu' k}$ signifies the inelastic tunneling amplitude. Since the molecular vibration does not contribute to the elastic current, we research the inelastic tunneling process only. By solving the time-dependent Schrödinger equation, we derive the inelastic tunneling current as follows,

$$I_{s,t} = \frac{2\pi e}{\hbar}\sum_{\nu,\nu'}\int_{-\infty}^{\mu_0} dE_n \int_{\mu_0}^{0} d\xi_k \rho_s(E_n)\rho_t(\xi_k)\mathcal{N}^2_{s,t}|_{E_n\to\xi_k} \times \langle\nu|\nu'\rangle^2\delta[E_{eg}+(\nu'-\nu)\hbar\omega+\xi_k+eV_b-E_n], \quad (17)$$

where μ_0 is the Fermi level of electrodes, with the assumption that the tip and the substrate are composed of the same metal. ρ_s and ρ_t denote the energy density of the state of the electron in the substrate and in the tip, respectively, which can be found in Ref. [39]. E_{eg} is the energy gap of the molecule. $\mathcal{N}_{s,t}|_{E_n\to\xi_k}$ represents the inelastic tunneling matrix element describing the process of the electrons tunneling from the substrate to the tip. It is written as follows,

$$\mathcal{N}_{s,t}|_{E_n\to\xi_k} = -e\vec{\mu}\cdot\langle\phi_k|\frac{\vec{r}}{|\vec{r}|^3}|\varphi_n\rangle, \quad (18)$$

where $|\phi_k\rangle$ and $|\varphi_n\rangle$ are the electronic wave functions in the tip and substrate regions, with their expressions shown as Eqs. (5) and (6), respectively. $\vec{r}$ is the position of the tunneling electron relative to the center of the molecule. By substituting the expression of the Franck-Condon factor into Eq. (17), we derive the expression of the inelastic current

$$I_{s,t} = \frac{2\pi e}{\hbar}\sum_{\nu'} e^{-S}\frac{S^{\nu'}}{\nu'!}\int_{-\infty}^{\mu_0} dE_n\int_{\mu_0}^{0} d\xi_k\rho_s(E_n)\rho_t(\xi_k) \times \mathcal{N}^2_{s,t}|_{E_n\to\xi_k}\delta(E_{eg}+\nu'\hbar\omega+\xi_k+eV_b-E_n). \quad (19)$$

This expression can be simplified due to the δ function. For convenience, we introduce the following definition:

$$\Delta = E_{eg}+\nu'\hbar\omega+eV_b. \quad (20)$$

Thus, the range of the integral alters with the value of Δ. When $\mu_0 < \Delta < 0$, the current is written as

$$I_{s,t} = \frac{2\pi e}{\hbar}\sum_{\nu'} e^{-S}\frac{S^{\nu'}}{\nu'!}\int_{\mu_0}^{\mu_0-\Delta} d\xi_k \times \rho_s(\xi_k+\Delta)\rho_t(\xi_k)\mathcal{N}^2_{s,t}|_{\xi_k+\Delta\to\xi_k}. \quad (21)$$

When $\Delta < \mu_0$, the current becomes

$$I_{s,t} = \frac{2\pi e}{\hbar}\sum_{\nu'} e^{-S}\frac{S^{\nu'}}{\nu'!}\int_{\mu_0}^{0} d\xi_k \times \rho_s(\xi_k+\Delta)\rho_t(\xi_k)\mathcal{N}^2_{s,t}|_{\xi_k+\Delta\to\xi_k}. \quad (22)$$

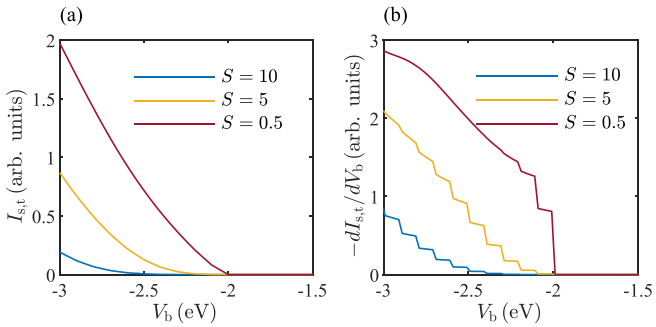

FIG. 1. (a) The inelastic tunneling current and (b) the differential conductance as a function of the bias voltage. The red (upper) curve, the yellow (middle) curve, and the blue (lower) curve correspond to vibronic coupling strengths with $S = 0.5$, $S = 5$, and $S = 10$, respectively. We have chosen parameters as $R = 0.5$ nm, $d = 0.5$ nm, $\vec{a} = (0, 0, d + R)$, $E_{eg} = 2$ eV, and $\mu_0 = -4.64$ eV. The characteristic frequency of the molecular vibration is fixed at 0.1 eV.

In experiments, both the elastic and the inelastic mechanisms contribute to the current spectrum. We can obtain the inelastic component via luminescence from the molecule. Once the molecule is excited to its excited state, it then decays back through the spontaneous emission process. We denote the molecular excitation probability as $p_e(t)$. The photon-counting rate is proportional to the probability in the excited state. The master equation of the excitation probability reads [26]

$$\frac{dp_e(t)}{dt} = -\gamma p_e(t) + \frac{I_{s,t}}{e}, \quad (23)$$

in which γ is the spontaneous decay rate. In the steady state, the photon-counting rate becomes

$$\Gamma = \frac{I_{s,t}}{e}. \quad (24)$$

Thus the inelastic tunneling current can be obtained from the photon-counting rate spectrum.

III. RESULTS

A. The inelastic tunneling current and the differential conductance

For numerical calculations of the inelastic tunneling current, we select silver (Ag) as the material for both the tip and the substrate. The Fermi level of silver is -4.64 eV. The characteristic frequency of the molecular vibration is assumed to be 0.1 eV. The distance between the tip and the substrate is set to $d = 0.5$ nm, and the radius of the apex atom of the tip is 0.5 nm. The tip is placed above the molecule. Taking the symmetry of the system into account, we express the position of the tip's apex as $\vec{a} = (0, 0, d + R)$. Furthermore, we choose different vibrational quantum numbers for the electronic excited state, ranging from 0 to 10. We also consider various cases with S, indicating different strengths of coupling between the vibration and electrons.

Figure 1 illustrates the behavior of the inelastic tunneling current (left figure) and the differential conductance (right figure) as a function of the bias voltage with various S equal to

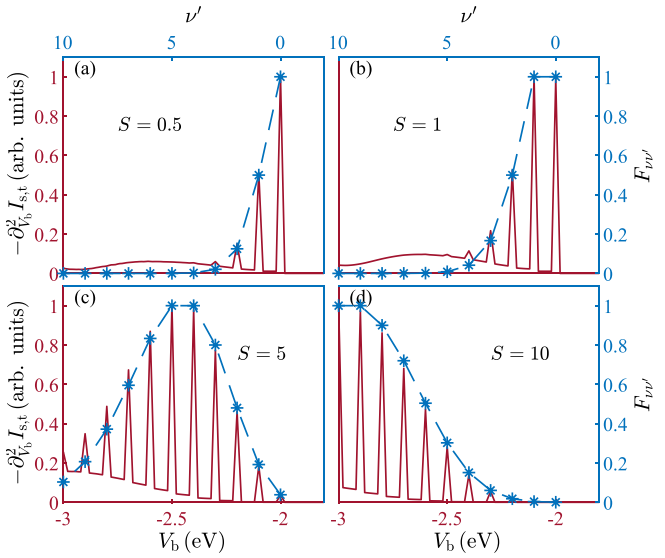

FIG. 2. The second derivative of the inelastic tunneling current with respect to the bias voltage (solid red line) and the Frank-Condon factor (blue asterisks) as a function of the bias voltage. (a)–(d) correspond to cases of $S = 0.5$, $S = 1$, $S = 5$, and $S = 10$, respectively. Parameters are the same as before.

0.5 (the upper red curve), 5 (the middle yellow curve), and 10 (the lower blue curve), respectively. In Fig. 1(a), the inelastic tunneling current increases as the bias voltage increases. The onset bias voltage differs among cases with different S because the vibronic coupling alters the molecular energy gap. Due to the Franck-Condon principle, a transition from one vibrational energy level to another is more likely to occur if the two vibrational wave functions overlap significantly. When the bias voltage reaches $-E_{eg} - [S]\hbar\omega$, where $[S]$ is the floor function and expressed as $[S] = \max\{n \in \mathbb{Z} | n \leqslant S\}$, the inelastic tunneling current and its differential conductance will exhibit a significant increase. In fact, $[S]\hbar\omega$ is associated with the Stokes shift in the emission spectra and the absorption spectra [25]. The stronger-coupling strength has a greater influence on the electronic transition process, leading to the smaller inelastic tunneling current. The curves of the differential conductance in Fig. 1(b) exhibit step structures. The spacing between these steps corresponds to the characteristic frequency $\hbar\omega$ of the molecular vibration.

B. Determining the Huang-Rhys factor

The solid red lines and the axes on the left and bottom sides of Fig. 2 illustrate the normalized second derivative of the inelastic tunneling current (denoted as $\partial^2_{V_b} I_{s,t}$) with respect to the bias voltage. Figures 2(a)–2(d) correspond to parameters with $S = 0.5$, $S = 1$, $S = 5$, and $S = 10$, respectively. These peaks in the graph represent the contribution of the vibration to the inelastic tunneling current. The width of these peaks is related to the numerical precision. It represents the broadening in energy level of molecules. From experimentally observed spectra, the order of magnitude of the width may be in the range of several tens of meV in metal-phthalocyanine molecules [3]. The blue asterisks and the axes on the right and top sides represent the normalized values of the Franck-Condon factor for integer values of ν' varying from 0 to 10 and $\nu = 0$. The dashed blue line connects these asterisks in sequence. For small values of ν', such as $\nu' = 0$ and $\nu' = 1$, the intensity of these peaks matches with blue asterisks, and the envelope of these peaks is consistent with the dashed blue line very well. Thus, for a given Huang-Rhys factor, the Franck-Condon factor effectively presents the character of the intensity of the second derivative of the inelastic tunneling current concerning the bias voltage.

From the expression of the inelastic tunneling current in Eq. (19), we can decompose $d^2I_{s,t}/dV_b^2$ spectra with the vibronic quantum number ν', and define $(d^2I_{s,t}/dV_b^2)_{\nu'}$ of the ν'th order as

$$\left(d^2I_{s,t}/dV_b^2\right)_{\nu'} = e^{-S}\frac{S^{\nu'}}{\nu'!}D_{\nu'}. \tag{25}$$

Here, the expression of the factor $D_{\nu'}$ is

$$D_{\nu'} = \frac{2\pi e}{\hbar}\frac{d^2}{dV_b^2}\int_{-\infty}^{\mu_0} dE_n \int_{\mu_0}^{0} d\xi_k \rho_s(E_n)\rho_t(\xi_k) \times \mathcal{N}^2_{s,t}|_{E_n\to\xi_k}\delta(E_{eg} + \nu'\hbar\omega + \xi_k + eV_b - E_n). \tag{26}$$

When the factor $D_{\nu'}$ changes with ν' as a slowly varying function, we get an approximate result about the ν'th order and the $(\nu' - 1)$th order of $d^2I_{s,t}/dV_b^2$ as

$$\frac{\left(d^2I_{s,t}/dV_b^2\right)_{\nu'}}{\left(d^2I_{s,t}/dV_b^2\right)_{\nu'-1}} \approx \frac{S}{\nu'}, \tag{27}$$

especially [40,41]

$$\frac{\left(d^2I_{s,t}/dV_b^2\right)_1}{\left(d^2I_{s,t}/dV_b^2\right)_0} \approx S. \tag{28}$$

The ratio of the intensity of the first order of $d^2I_{s,t}/dV_b^2$ to the zeroth order of $d^2I_{s,t}/dV_b^2$ is approximately equal to the Huang-Rhys factor. This conclusion provides a theoretical foundation for experimental determination of the Huang-Rhys factor. Once the inelastic tunneling current is obtained, we can analyze its second derivative with respect to the bias voltage, from which the oscillation quantum number ν' can be obtained. Also, the interval between peaks gives the value of the vibronic frequency ω. Through the intensity of these peaks with the first order and the zeroth order, we calculate the Huang-Rhys factor. When dealing with cases where electronic excitation is coupled with various vibrational degrees of freedom, this method may give the Huang-Rhys factors with the corresponding vibrational modes.

The method we propose involves decomposing the $d^2I_{s,t}/dV_b^2$ spectra and approximating the Huang-Rhys factor with the value of $(d^2I_{s,t}/dV_b^2)_1/(d^2I_{s,t}/dV_b^2)_0$. To verify the validity of the method, Fig. 3 illustrates results estimated from Eq. (28) as a function of the true value of S. The red line is linear and represents the true value of S in the ideal situation without any approximation. Blue circles represent the estimated results from the left-hand side of Eq. (28) with different vibronic coupling strengths, corresponding to cases of $S = 0.1$, $S = 0.5$, $S = 1$, $S = 5$, and $S = 10$, respectively. The coincidence between blue circles and the red line proves

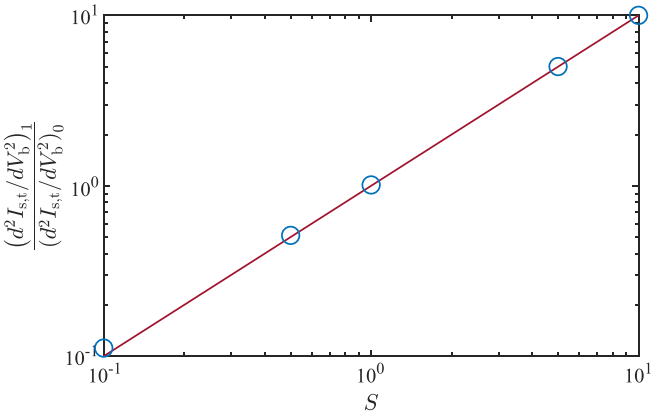

FIG. 3. The comparison of the estimated value of S from Eq. (28) with the true value of S. The red line is linear and represents the true value of S. The blue circles are the estimated values from the left-hand side of Eq. (28), corresponding to cases of $S = 0.1$, $S = 0.5$, $S = 1$, $S = 5$, and $S = 10$, respectively.

the validity of the approximate results obtained from Eq. (28). There is a slight deviation between the estimated values and the true values in the case of weak vibronic coupling. However, in cases of the strong vibronic coupling, the estimated value matches the true S very well. This figure shows that $D_{\nu'}$ is a slowly varying function, and Eq. (28) can be effectively used to determine the Huang-Rhys factor of the molecule.

IV. CONCLUSION

We have studied the STML system, where the molecule is modeled as a two-level system with a molecular vibration degree of freedom. Based on Bardeen's theory, the inelastic tunneling current is expressed in terms of the Huang-Rhys factor S. Information regarding vibronic coupling is obtained from the differential conductance, which exhibits steps as a function of the bias voltage. The Huang-Rhys factor is determined from the second derivative of the inelastic tunneling current with respect to the bias voltage. Our study focuses on the IES mechanism in STML, where the Huang-Rhys factor of a single molecule is approximated by $d^2I_{s,t}/dV_b^2$ spectra. The method involving the analysis of the inelastic tunneling current in STML will provide an alternative approach for determining the Huang-Rhys factor.

ACKNOWLEDGMENTS

This work is supported by the Innovation Program for Quantum Science and Technology (Grant No. 2023ZD0300700), and the National Natural Science Foundation of China (Grants No. U2230203, No. U2330401, No. 12088101, and No. 12205211).

[1] X. H. Qiu, G. V. Nazin, and W. Ho, Vibrationally resolved fluorescence excited with submolecular precision, Science **299**, 542 (2003).

[2] F. Schwarz, Y. F. Wang, W. A. Hofer, R. Berndt, E. Runge, and J. Kröger, Electronic and vibrational states of single tin–phthalocyanine molecules in double layers on Ag(111), J. Phys. Chem. C **119**, 15716 (2015).

[3] X. H. Qiu, G. V. Nazin, and W. Ho, Vibronic states in single molecule electron transport, Phys. Rev. Lett. **92**, 206102 (2004).

[4] S. W. Wu, N. Ogawa, G. V. Nazin, and W. Ho, Conductance hysteresis and switching in a single-molecule junction, J. Phys. Chem. C **112**, 5241 (2008).

[5] C. Chen, P. Chu, C. A. Bobisch, D. L. Mills, and W. Ho, Viewing the interior of a single molecule: Vibronically resolved photon imaging at submolecular resolution, Phys. Rev. Lett. **105**, 217402 (2010).

[6] Y. Zhang, Y. Luo, Y. Zhang, Y.-J. Yu, Y.-M. Kuang, L. Zhang, Q.-S. Meng, Y. Luo, J.-L. Yang, Z.-C. Dong, and J. G. Hou, Visualizing coherent intermolecular dipole–dipole coupling in real space, Nature (London) **531**, 623 (2016).

[7] G. V. Nazin, X. H. Qiu, and W. Ho, Visualization and spectroscopy of a metal-molecule-metal bridge, Science **302**, 77 (2003).

[8] L. Zhang, Y.-J. Yu, L.-G. Chen, Y. Luo, B. Yang, F.-F. Kong, G. Chen, Y. Zhang, Q. Zhang, Y. Luo, J.-L. Yang, Z.-C. Dong, and J. G. Hou, Electrically driven single-photon emission from an isolated single molecule, Nat. Commun. **8**, 580 (2017).

[9] K. Miwa, H. Imada, M. Imai-Imada, K. Kimura, M. Galperin, and Y. Kim, Many-body state description of single-molecule electroluminescence driven by a scanning tunneling microscope, Nano Lett. **19**, 2803 (2019).

[10] F.-F. Kong, X.-J. Tian, Y. Zhang, Y.-J. Yu, S.-H. Jing, Y. Zhang, G.-J. Tian, Y. Luo, J.-L. Yang, Z.-C. Dong, and J. G. Hou, Probing intramolecular vibronic coupling through vibronic-state imaging, Nat. Commun. **12**, 1280 (2021).

[11] R. J. Peña Román, D. Pommier, R. Bretel, L. E. Parra López, E. Lorchat, J. Chaste, A. Ouerghi, S. Le Moal, E. Boer-Duchemin, G. Dujardin, A. G. Borisov, L. F. Zagonel, G. Schull, S. Berciaud, and E. Le Moal, Electroluminescence of monolayer WS_2 in a scanning tunneling microscope: Effect of bias polarity on spectral and angular distribution of emitted light, Phys. Rev. B **106**, 085419 (2022).

[12] F. Wen, G. Dong, and H. Dong, Measuring fine molecular structures with luminescence signal from an alternating current scanning tunneling microscope, Commun. Theor. Phys. **74**, 125105 (2022).

[13] B. C. Stipe, M. A. Rezaei, and W. Ho, Single-molecule vibrational spectroscopy and microscopy, Science **280**, 1732 (1998).

[14] B. C. Stipe, M. A. Rezaei, and W. Ho, Coupling of vibrational excitation to the rotational motion of a single adsorbed molecule, Phys. Rev. Lett. **81**, 1263 (1998).

[15] L. J. Lauhon and W. Ho, Single-molecule vibrational spectroscopy and microscopy: CO on Cu(001) and Cu(110), Phys. Rev. B **60**, R8525 (1999).

[16] N. Lorente and M. Persson, Theory of single molecule vibrational spectroscopy and microscopy, Phys. Rev. Lett. **85**, 2997 (2000).

[17] N. A. Pradhan, N. Liu, and W. Ho, Vibronic spectroscopy of single C_{60} molecules and monolayers with the STM, J. Phys. Chem. B **109**, 8513 (2005).

[18] G. V. Nazin, S. W. Wu, and W. Ho, Tunneling rates in electron transport through double-barrier molecular junctions in a scanning tunneling microscope, Proc. Natl. Acad. Sci. USA **102**, 8832 (2005).

[19] K. Huang and A. Rhys, Theory of light absorption and non-radiative transitions in *F*-centres, Proc. R. Soc. London, Ser. A **204**, 406 (1950).

[20] A. M. Lemos and J. J. Markham, Calculation of the Huang-Rhys factor for *F*-centers, J. Phys. Chem. Solids **26**, 1837 (1965).

[21] E. Mulazzi and N. Terzi, Evaluation of the Huang-Rhys factor and the half-width of the F-band in KCl and NaCl crystals, J. Phys. Colloq. **28**, C4-49 (1967).

[22] M. Moreno, M. T. Barriuso, and J. A. Aramburu, The Huang-Rhys factor $S(a_{1g})$ for transition-metal impurities: a microscopic insight, J. Phys.: Condens. Matter **4**, 9481 (1992).

[23] A. Schenk, A model for the field and temperature dependence of Shockley-Read-Hall lifetimes in silicon, Solid-State Electron. **35**, 1585 (1992).

[24] L. Razinkovas, M. W. Doherty, N. B. Manson, C. G. Van de Walle, and A. Alkauskas, Vibrational and vibronic structure of isolated point defects: The nitrogen-vacancy center in diamond, Phys. Rev. B **104**, 045303 (2021).

[25] M. de Jong, L. Seijo, A. Meijerink, and F. T. Rabouw, Resolving the ambiguity in the relation between Stokes shift and Huang–Rhys parameter, Phys. Chem. Chem. Phys. **17**, 16959 (2015).

[26] G. Dong, Y. You, and H. Dong, Microscopic origin of molecule excitation via inelastic electron scattering in scanning tunneling microscope, New J. Phys. **22**, 113010 (2020).

[27] G. Dong, Z. Hu, X. Sun, and H. Dong, Structural reconstruction of optically invisible state in a single molecule via scanning tunneling microscope, J. Phys. Chem. Lett. **12**, 10034 (2021).

[28] D. Drakova and G. Doyen, Local charge injection in STM as a mechanism for imaging with anomalously high corrugation, Phys. Rev. B **56**, R15577 (1997).

[29] M. Galperin and A. Nitzan, Current-induced light emission and light-induced current in molecular-tunneling junctions, Phys. Rev. Lett. **95**, 206802 (2005).

[30] U. Harbola, J. B. Maddox, and S. Mukamel, Many-body theory of current-induced fluorescence in molecular junctions, Phys. Rev. B **73**, 075211 (2006).

[31] S. Jiang, T. Neuman, R. Bretel, A. Boeglin, F. Scheurer, E. Le Moal, and G. Schull, Many-body description of STM-induced fluorescence of charged molecules, Phys. Rev. Lett. **130**, 126202 (2023).

[32] B. Doppagne, M. C. Chong, E. Lorchat, S. Berciaud, M. Romeo, H. Bulou, A. Boeglin, F. Scheurer, and G. Schull, Vibronic spectroscopy with submolecular resolution from STM-induced electroluminescence, Phys. Rev. Lett. **118**, 127401 (2017).

[33] A. Martín-Jiménez, A. I. Fernández-Domínguez, K. Lauwaet, D. Granados, R. Miranda, F. J. García-Vidal, and R. Otero, Unveiling the radiative local density of optical states of a plasmonic nanocavity by STM, Nat. Commun. **11**, 1021 (2020).

[34] J.-Z. Zhu, G. Chen, T. Ijaz, X.-G. Li, and Z.-C. Dong, Influence of an atomistic protrusion at the tip apex on enhancing molecular emission in tunnel junctions: A theoretical study, J. Chem. Phys. **154**, 214706 (2021).

[35] K. Miwa, S. Sakamoto, and A. Ishizaki, Control and enhancement of single-molecule electroluminescence through strong light–matter coupling, Nano Lett. **23**, 3231 (2023).

[36] J. Bardeen, Tunnelling from a many-particle point of view, Phys. Rev. Lett. **6**, 57 (1961).

[37] J. Franck and E. G. Dymond, Elementary processes of photochemical reactions, Trans. Faraday Soc. **21**, 536 (1926).

[38] E. Condon, A theory of intensity distribution in band systems, Phys. Rev. **28**, 1182 (1926).

[39] D. A. Papaconstantopoulos, *Handbook of the Band Structure of Elemental Solids: From $Z = 1$ To $Z = 112$*, 2nd ed. (Springer, Berlin, 2015).

[40] S. J. Xu, W. Liu, and M. F. Li, Direct determination of free exciton binding energy from phonon-assisted luminescence spectra in GaN epilayers, Appl. Phys. Lett. **81**, 2959 (2002).

[41] S.-J. Xu, Huang-Rhys factor and its key role in the interpretation of some optical properties of solids, Acta Phys. Sin. **68**, 166301 (2019).